Proc. Natl. Conf. Theor. Phys. **37** (2012), pp. 49-58

CHIRAL PHASE TRANSITION IN COMPACTIFIED SPACE-TIME

TRAN HUU PHAT[1], NGUYEN VAN THU[2]
[1] *Vietnam Atomic Energy Commission, 59 Ly Thuong Kiet, Hanoi, Vietnam and Dong Do University, 8 Nguyen Cong Hoan, Hanoi, Vietnam*
[2] *Department of Physics, Hanoi University of Education II, Hanoi, Vietnam*

Abstract. *The chiral phase transition of linear sigma model with constituent quarks at finite temperature T and chemical potential μ is scrutinized in a non-simply connected space-time where the compactified dimension with length L is taken along the Oz direction. It results that corresponding to untwisted and twisted quarks the phase diagrams in the (T, L^{-1})- plane are quite different from each other. Here, untwisted (twisted) quark denotes the quark field which satisfies the periodic (anti-periodic) boundary conditions. In the chiral limit the chiral phase transition for untwisted quark is first order for all values of L, while for twisted quark it is first order at high L and becomes second order at lower values of L . In the physical world with explicit symmetry breaking, it is found that the chiral phase transition for untwisted quark is first order at low values of L and eventually ends up with a critical end point at high L, and for twisted quark it is a crossover transition everywhere.*

I. INTRODUCTION

Motivated by the early work of Kaluza and Klein [1] who attempted to unify gravity with other forces in nature the study of physical phenomena arising in a space-time with nontrivial topology has attracted many investigators in recent years. There, the extra spatial dimension was introduced and compactified in small distances. The physical theories with compactified spatial dimensions are developed in diverse domains of modern physics:

1- This idea has been intensively developed with different applications in supergravity, superstrings and brane theories [2]. Especially, extra dimensions have been extended to lower energy scale for understanding the hierarchy between mass scales existing in high energy physics [3, 4].

2- The holographic QCD [5], the holographic nuclear theory [6] and the holographic theory of high temperature superconductor [7] have been proposed and developed with great interest. Here, based on the gauge/gravity duality [8] the gauge theory is transferred to the gravitation theory in the higher - dimensional space-time with some compactifications. As consequence, the problem of non-perturbative nature is hopefully solved by means of the perturbative method of the gravity theory.

3- On the other hand, it is well known that the space-time with nontrivial topology can give rise to new physical effects, such as the celebrated Casimir effect [9, 10], caused by the vacuum structure of quantized field restricted in a domain of compactified space-time. The Casimir energy and its role in cosmology have been explored in Refs.[11]-[17], in particular, it was employed to model the dark energy for explaining the present accelerated expansion of universe [11, 12]. In condensed matter physics the Casimir effect is applied not

only to the fabrication and operation of nano - scale systems [18], but also to nanophysics [19, 20] since the single-walled carbon nanotubes are generated by graphene sheet and the background space-time for corresponding Dirac-like theory of the electronic states in grapheme has topology $S^1 \times R^2$.

Following the idea of compactified spatial dimensions this paper is devoted to the study of chiral phase transition in the space-time with topology $S^1 \times R^3$, in which the Casimir effect is not taken into account. We start from the linear sigma model involving constituent quarks, whose Lagrangian reads

$$\mathcal{L} = \mathcal{L}_{LSM} + \overline{q}\left[i\gamma^\mu\partial_\mu - m_q - g(\sigma + i\gamma^5\vec{\tau}\vec{\pi})\right]q + \mu\overline{q}\gamma^4 q, \tag{1}$$

in which

$$\mathcal{L}_{LSM} = \frac{1}{2}\left[\partial_\alpha\sigma\partial^\alpha\sigma + \partial_\alpha\vec{\pi}\partial^\alpha\vec{\pi}\right] - U,$$
$$U = \frac{m^2}{2}(\sigma^2 + \vec{\pi}^2) + \frac{\lambda^2}{4}(\sigma^2 + \vec{\pi}^2)^2 - \epsilon f_\pi m_\pi^2\sigma,$$

where q, σ and $\vec{\pi}$ denote respectively the quark, sigma and pion fields; μ is the quark chemical potential; g, m and λ are the coupling constants, m_q is current quark mass and $\epsilon = 0, 1$. The coupling constants are determined

$$m^2 = \frac{3m_\pi^2 - m_\sigma^2}{2} < 0,\ \lambda^2 = \frac{m_\sigma^2 - m_\pi^2}{2f_\pi^2} > 0.$$

The present article is organized as follows. In Section II we calculate the effective potential and gap equations for both untwisted and twisted quarks and study numerically the chiral phase transition. The conclusion and discussion are given in Section III.

II. CHIRAL PHASE TRANSITION WITHOUT CASIMIR EFFECT

II.1. The effective potential and gap equation

After a Wick rotation the classical action S_E corresponding to (1) reads

$$S_E = i\int_0^L dx_3\int_{-\infty}^{+\infty} d\tau dx_\perp \mathcal{L}_E. \tag{2}$$

In the mean - field approximation σ and $\vec{\pi}$ develop the ground - state expectation values

$$\langle\sigma\rangle = u,\ \langle\vec{\pi}\rangle = 0.$$

As known [21, 22], the non - trivial topology of space-time leads to the existence of two types of boundary conditions for quark fields that are either periodic (untwisted quark) or anti - periodic (twisted quark)

$$q(\tau, x, y, z = 0) = \pm q(\tau, x, y, z = L). \tag{3}$$

As is indicated in (3) there is a similarity between L and $\beta = 1/T$ in the Matsubara formalism.

Next the grand partition function is established

$$Z = \int \mathcal{D}\overline{q}\mathcal{D}q \exp[-S_E],$$

which, taking into account (3), leads to the effective potential

$$\Omega(u, L) = -\frac{\ln Z}{VL} = U + \Omega_{q\overline{q}}, \tag{4}$$

where V means the volume of the Euclidean 3 - dimensional space - time and

$$\Omega_{q\overline{q}} = -\frac{\nu_q}{L}\sum_{n=-\infty}^{+\infty}\int\frac{d\vec{p}_\perp}{(2\pi)^2}\left\{E_n + T\ln\left[1+\exp\left(-\frac{E_n-\mu}{T}\right)\right] + T\ln\left[1+\exp\left(-\frac{E_n+\mu}{T}\right)\right]\right\}, \tag{5}$$

with

$$E_n = \sqrt{p_{3n}^2 + p_\perp^2 + M^2},$$
$$M = m_q + gu.$$

The first term under the integral is exactly the vacuum contribution, which is relevant to the Casimir energy. We first discard it temporarily, then the expression is simplified to

$$\Omega_{q\overline{q}} = -\frac{\nu_q T}{L}\sum_{n=-\infty}^{+\infty}\int\frac{d\vec{p}_\perp}{(2\pi)^2}\left\{\ln\left[1+\exp\left(-\frac{E_n-\mu}{T}\right)\right] + \ln\left[1+\exp\left(-\frac{E_n+\mu}{T}\right)\right]\right\}. \tag{6}$$

The boundary conditions (3) yield

$$p_{3n} = \frac{2n\pi}{L}, \tag{7}$$

for untwisted quark and

$$p_{3n} = \frac{(2n+1)\pi}{L}, \tag{8}$$

for twisted quark.

The ground state of the system is determined by

$$\frac{\partial\Omega}{\partial u} = 0,$$

or

$$m^2 u + \lambda^2 u^3 - \epsilon f_\pi m_\pi^2 + \frac{\partial\Omega_{q\overline{q}}}{\partial u} = 0, \tag{9}$$

where

$$\frac{\partial\Omega_{q\overline{q}}}{\partial u} = \frac{\nu_q}{L} gM \sum_{n=-\infty}^{+\infty}\int\frac{d\vec{p}_\perp}{(2\pi)^2}\times\frac{1}{E_n}\left\{\frac{1}{e^{(E_n-\mu)/T}+1} + \frac{1}{e^{(E_n+\mu)/T}+1}\right\}. \tag{10}$$

Eqs.(9), (10) together with (7) and (8) are called the gap equations for untwisted and twisted quarks, respectively. They play the essential role in what follows.

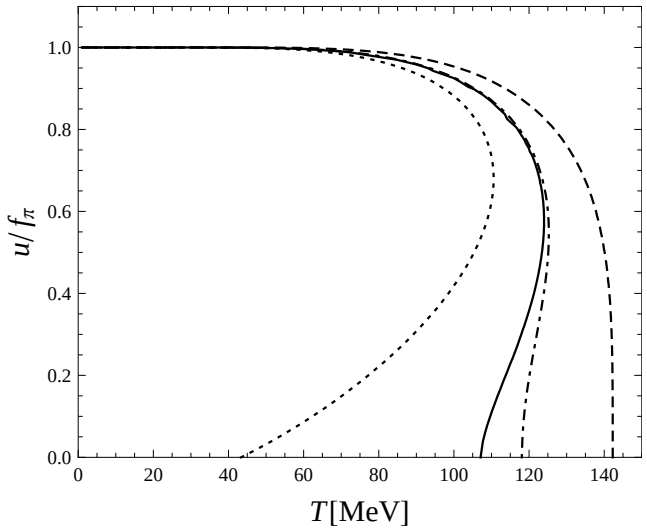

Fig. 1. In the chiral limit and $\mu = 0$. The evolution of chiral condensate as a function of T. The solid line corresponds to $L \to \infty$ for both twisted and untwisted quarks. The dashed (dashed-dotted) line corresponds to twisted quark at L = 1.973fm (3.946 fm). The dotted line corresponds to untwisted quark at $L = 1.973$ fm.

II.2. Numerical study

In order to proceed to the numerical computation the model parameters are chosen to be $m_\sigma = 500$ MeV, $m_\pi = 138$ MeV, $f_\pi = 93$ MeV, $m_q = 5.5$ MeV and therefore the value $g = 3.3$ provides the mass of constituent quark.

With the aid of MATHEMATICA [23] and FORTRAN we will investigate the chiral phase structure for the following cases:

II.2.1. *In the chiral limit,* $\epsilon = 0$ *and* $m_q = 0$

Let us first consider the case when $\mu = 0$. Then based on Eqs. (7), (8) and (9) it is found that

- The evolution of chiral condensate $u(T, L)$ versus T at several values of L are depicted in Fig.1 for both twisted and untwisted quarks. It is evident that for untwisted quark the phase transition is always first - order, while for twisted quark the transition is first - order for $L > 1.972$ fm and becomes second - order for smaller L.

The statement that the transition is first - order for untwisted quark at several values of L is easily tested by observing the evolution of effective potential Ω versus u at $\mu = 0$ and $L = 3.946$ fm shown in Fig.2. It is found that two minima of Ω exhibit as degenerate at the critical temperature $T_c = 117.38$ MeV. Analogously, the first - order transition for twisted quark in the interval $1.972\text{fm} \leq L \leq \infty$ is also confirmed.

- As a consequence, the phase diagrams in the (T, L^{-1}) - plane are plotted by upper lines in Fig.3(a) (for untwisted quark) and Fig.3(b) (for twisted quark).

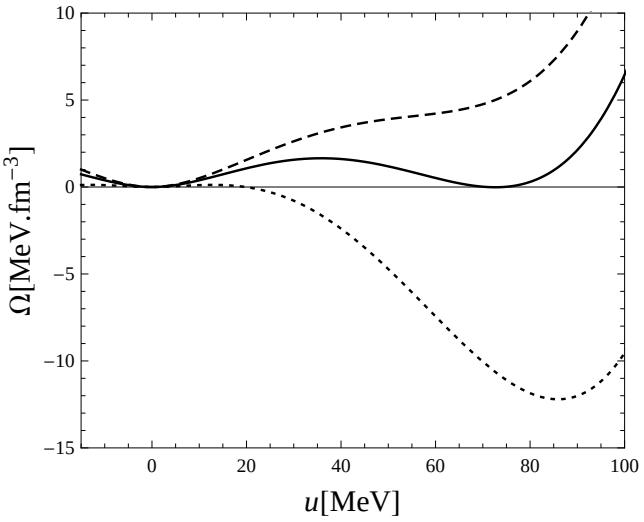

Fig. 2. In the chiral limit and for untwisted quark. The evolution of effective potential versus u at $\mu = 0, L = 3.946$ fm and $T = 100$ MeV (dotted line), $T = 117.83$ MeV (solid line) and $T = 125$ MeV (dashed line).

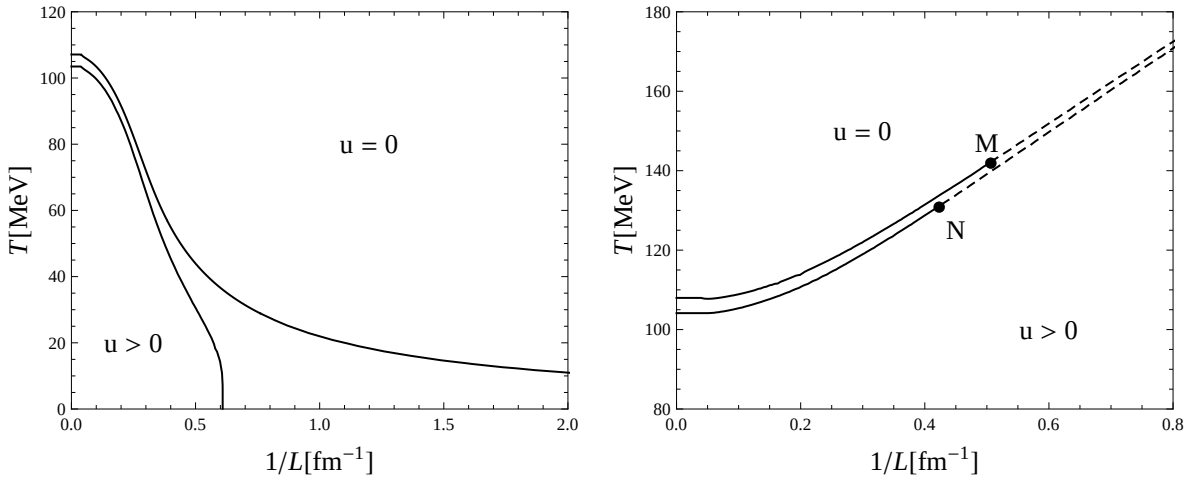

(a) untwisted quark (b) twisted quark

Fig. 3. In the chiral limit. The phase diagram of chiral condensate in (T, L^{-1}) - plane at $\mu = 0$ (upper line) and $\mu = 50$ MeV (lower line). The solid line denotes first - order phase transition.

Next the case $\mu = 50$ MeV is concerned. Solving Eqs. (7) - (10) together with

$$u(T, \mu = 50\text{MeV}, L) = 0,$$

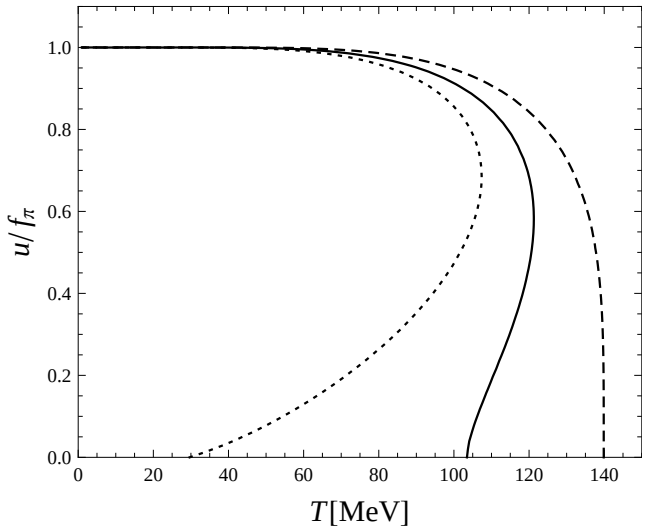

Fig. 4. In the chiral limit and $\mu = 50$ MeV. The evolution of chiral condensate as a function of T. The solid line corresponds to $L \to \infty$ for both twisted and untwisted quarks. The dashed and dotted lines correspond to twisted and untwisted quarks and $L = 1.973$ fm.

leads to the phase diagrams plotted by lower lines in Fig.3(a) and Fig.3(b). The order of the transition is determined from the evolution of chiral condensate versus T at several values of L for each case. With this in mind we obtain Fig.3 which yield the scenarios: for untwisted quark the transition is first - order everywhere, whereas for twisted quark the chiral phase transition changes from first - order at $L > 2.358$ fm to second - order at smaller L. Two types of transitions are separated by a tri - critical point.

II.2.2. *In the physical world,* $\epsilon = 1$ *and* $m_q = 5.5$ *MeV*

We will consider in this part the phase diagrams in the (T, L^{-1}) - plane corresponding to $\mu = 0$ and 200 MeV, respectively.

a- Solving the gap equations, Eqs.(7), (9) and (10), for untwisted quark generates the solid and dotted lines in Fig.5(a) ($\mu = 0$) and Fig.5(b) ($\mu = 200$ MeV), which represent the T dependence of chiral condensate at several values of L. Their common feature is that every figure has two different regions of temperature, separated by a definite value $T = T_0$ (of course, T_0 depends on μ) so that for $T > T_0$ the order parameter u is a single - valued function of T and smoothly tends to zero as T increases. This kind of behavior of u is usually defined as a crossover transition. Meanwhile, for $T < T_0$ the order parameter turns out to be multi - valued function of T, where, owing to Asakawa and Yazaki [24], a first - order phase transition emerges. Then applying their proposed method, which essentially identifies the multi - valued region of chiral condensate to the region of first - order phase transition, we are led to the phase diagram in the (T, L^{-1}) - plane plotted in Fig.6(a) for $\mu = 0$ and $\mu = 200$ MeV. Here, the solid lines (dashed lines) denote first - order phase transition (crossover transition). In each diagram two types of transitions are separated by a critical end point (CEP).

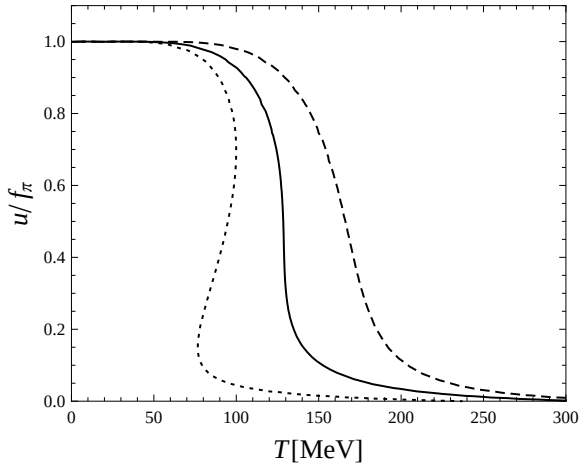

(a) $\mu = 0$, the dashed and dotted lines correspond to twisted and untwisted quarks and $L = 1.316$ fm.

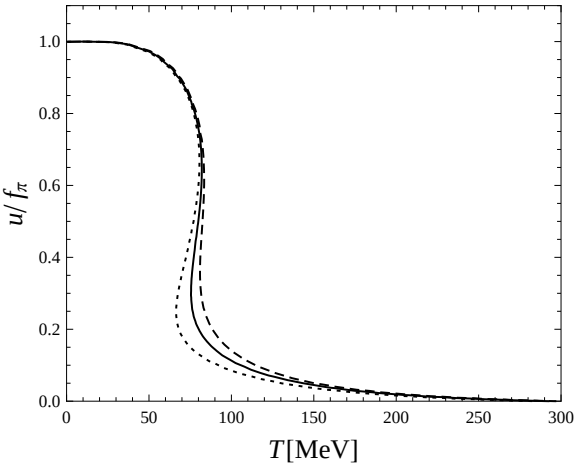

(b) $\mu = 200$ MeV, the dashed and dotted lines correspond to twisted and untwisted quarks and $L = 39.46$ fm.

Fig. 5. The evolution of chiral condensate as a function of T. The solid line corresponds to $L \to \infty$ for both twisted and untwisted quarks.

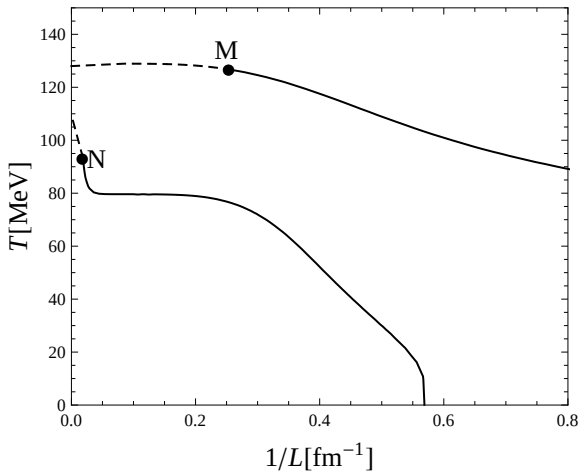

(a) untwisted quark

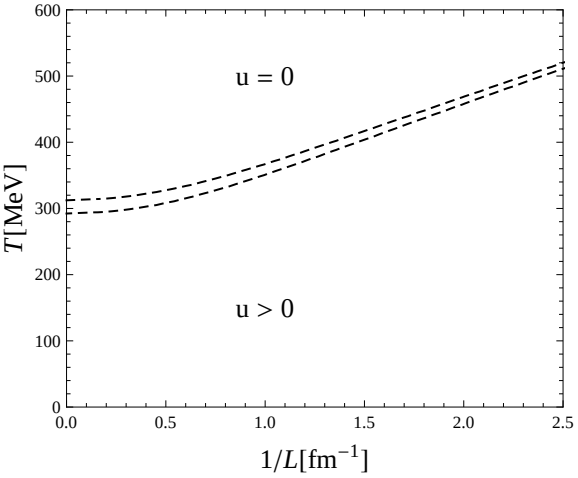

(b) twisted quark

Fig. 6. The phase diagram of chiral condensate in (T, L^{-1}) - plane. From the top to bottom the graphs correspond to $\mu = 0, 200$ MeV. The solid line means first - order phase transition and dashed line means crossover transition. M, N are the CEPs with corresponding coordinates $(T, L) =$ (126.72 MeV, 3.953 fm) and (93.37 MeV, 55.56 fm).

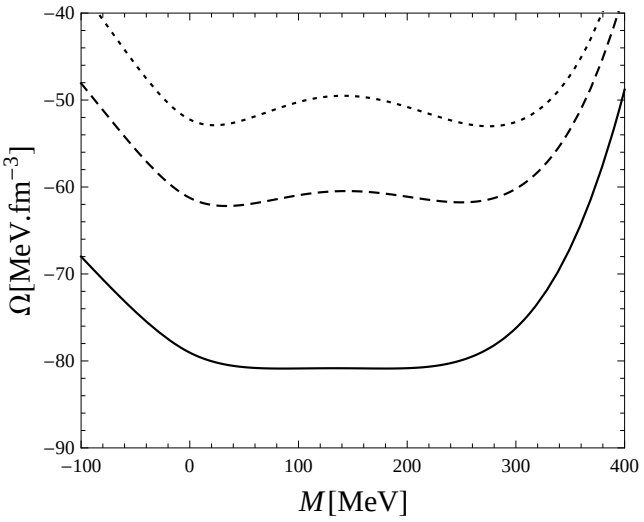

Fig. 7. The evolution of effective potential versus M at $\mu = 0$ in the physical world and for untwisted quark. Starting from the top, the graphs correspond to (T, L) = (92.1 MeV, 1.318 fm), (109.446 MeV, 1.972 fm), (126.721 MeV, 3.953 fm).

It is important to remember that solving the gap equation is not sufficient to decide the order of the transition [25], therefore this result is reconfirmed only when we consider additionally the evolution of the effective potential versus M for several values of (T, L) belonging to the multi - valued region of chiral condensate. They are depicted in Fig.7 for $\mu = 0$, featured by the fact that at critical temperature $T = T_c$ (of course, T_c depends on μ) the first - order phase transition is expressed by dotted lines with two minima corresponding to restored and broken symmetry, separated by a barrier. As T increases the barrier smears out and at $T = T_{cross}$ (evidently, T_{cross} depends on μ, too) the barrier disappears, signaling the onset of a crossover transition. We also obtain at $\mu = 200$ MeV the similar scenario.

b- Concerning twisted quark we plot the solid and dashed lines in Fig.5(a) ($\mu = 0$) and Fig.5(b) ($\mu = 200$ MeV) the T dependences of chiral condensate at several L steps. It is clear that as T increases the chiral condensate always smoothly goes to zero. This implies that the chiral transition for different cases is of crossover type everywhere. The corresponding phase diagrams $u(T, L) = 0$ in the (T, L^{-1}) - plane are represented in Fig.6(b), from the top to bottom the graphs correspond to $\mu = 0$ and $\mu = 200$ MeV.

III. CONCLUSION AND DISCUSSION

The most important results we found in this paper are in order:

a- Pions are split up into untwisted and twisted pions with quite different masses when moving in restricted domain of space-time.

b- The finite-size effect indicates that the critical temperature monotonously increases as L decreases in the twisted-quark case. This effect is of great significance for

applying to high-temperature superconductors and ultrathin films of superconducting metals. Indeed, similarly to quarks, electrons which formed Cooper pairs could be split up into untwisted and twisted electrons. So, it is probable that the systems might turn out to be high-temperature superconductors with two energy gaps: the first gap corresponds to untwisted-electron pairs and the second gap to twisted-electron pairs. The critical temperature of normal-superconducting phase transition becomes high when L is sufficiently small.

All new phenomena mentioned above are very interesting. Their experimental confirmations are related to a more fundamental problem which arises is that how to discover experimentally the existences of two types of fermions in real systems when space-time is compactified. Perhaps, the physics of ultracold gases is most suited for this purpose. We know that at ultracold temperature the strength of inter-atomic interaction is characterized by scattering length a. Across the Feshbach resonance, in principle, a^{-1} can be tuned to any value, from $-\infty$ to $+\infty$. Therefore, by means of ultracold gases we are able to study quantum physics of interacting fermions from weak to strong couplings. Here, experimental realization could prove whether or not both untwisted-fermion and twisted-fermion condensates coexist in quasi two-dimensional space.

ACKNOWLEDGMENT

This paper is financially supported by the Vietnam National Foundation for Science and Technology Development (NAFOSTED).

REFERENCES

[1] See, for example, *Modern Kaluza-Klein theories*, edited by T. Appelquits, A. Chodos and P. T. O Freund (Addison-Wesley, Reading, MA, 1987).
[2] J. H. Schwarz, astro-ph/0304507.
[3] N. Arkani-Hamed, S. Dimopoulos and G. Dvali, Phys. Lett. B **429**, 263 (1998); ibid. Phys. Rev. D **59**, 086004 (1999).
[4] L. Randall and R. Sundrum, Phys. Rev. Lett. **83**, 3370 (1999); ibid. **83**, 4690 (1999).
[5] T. Sakai and S. Sugimoto, Prog. Theor. Phys. **113**, 843 (2005) (hep-th/0412141); ibid. **114**, 1083 (2005) (hep-th/0507073).
[6] O. Bergman, G. Lifschytz and M. Lipper, *Holographic Nuclear Physics*, JHEP **0711**, 056 (2007) (hep-th/0708.0326); M. Rozali, H. H. Shieh, M. van Raamsdonk, J. Wu, *Cold Nuclear Matter in Holographic QCD*, JHEP **0801**, 053 (2008) (hep-th/0708.1322).
[7] G. T. Horowitz, *Introduction to holographic superconductors*, arxiv:1002.1722.
[8] J. M. Maldacena, Adv. Theor. Math. Phys. **2**, 231 (1998) (hep-th/9711200).
[9] H. B. G. Casimir, Proc. K. Ned. Akad. Wet. **51**, 793 (1948).
[10] M. Bordag, V. Mohideen and V. M. Mostepanenko, Phys. Rep. **353**, 1 (2001).
[11] E. Elizalde, S. Nojiri and S. D. Odintsov, Phys. Rev. D **70**, 043539 (2004).
[12] E. Elizalde, J. Phys. A **39**, 6299 (2006).
[13] V. M. Mostepanenko and N. N. Trunov, *The Casimir Effect and Its Applications* (Clarendon, Oxford, 1997).
[14] E. Elizalde, S. D. Odintsov, A. Romeo, A. A. Bytsenko and S. Zerbini, *Zeta Regularization Techniques with Applications* (World Scientific, Singapore, 1994).
[15] K. A. Milton, *The Casimir Effect:Physical Manifestation of Zero-Point Energy* (World Scientific, Singapore, 2002).

[16] M. Bordag, G. L. Klimchitskaya, U. Mohideen and V. M. Mostepanenko, *Advances in the Casimir Effect* (Oxford University Press, Oxford, 2009).
[17] A. A. Bytsenko, G. Cognola, L.Vanzo and S. Zerbini, Phys. Rep. **266**, 1 (1996).
[18] E. Buks and M. L. Roukes, Phys. Rev. B **63**, 033402 (2001); C. Genet, A. Lambrecht and S. Reynaud, Eur. Phys. J. Special Topics **160**, 183 (2008).
[19] R. Saito, G. Dresselhaus and M. S. Dresselhaus, *Physical Properties of Carbon Nanotubes* (Imperial College Press, London, 1998); C. Dupas, P. Houdy and M. Lahmani, *Nanoscience: Nanotechnologies and Nanophysics* (Springer, Berlin, 2007).
[20] A. H. Castro Neto, F. Guinea , N. M. R. Peres, K. S. Novoselov and A. K. Geim, Rev. Mod. Phys. **81**, 109 (2009).
[21] C. J. Isham, Proc. R. Soc. London A **362**, 383 (1978); ibid. **364**, 591 (1978).
[22] L. H. Ford, Phys. Rev. D **21**, 949 (1980).
[23] S. Wolfram, *The Mathematica Book*, 5th edition, (Wolfram Media, Champaign, Illinos, 2003).
[24] M. Asakawa and K. Yazaki, Nucl. Phys. A **504**, 668 (1989).
[25] M. Buballa, Phys. Rep. **407**, 205 (2005).

Received 30-09-2012.